

# Soliton assisted control of source to drain electron transport along natural channels – crystallographic axes – in two-dimensional triangular crystal lattices

A.P. Chetverikov<sup>1,2</sup>, W. Ebeling<sup>1,3</sup>, and M.G. Velarde<sup>1,a</sup>

<sup>1</sup> Instituto Pluridisciplinar, Universidad Complutense, Paseo Juan XXIII, 1, 28040 Madrid, Spain

<sup>2</sup> Department of Physics, Saratov State University, Astrakhanskaya 83, 410012 Saratov, Russia

<sup>3</sup> Institut für Physik, Humboldt-Universität Berlin, Newtonstrasse 15, 12489 Berlin, Germany

Received 7 March 2016 / Received in final form 7 July 2016

Published online 12 September 2016 – © EDP Sciences, Società Italiana di Fisica, Springer-Verlag 2016

**Abstract.** We present computational evidence of the possibility of fast, supersonic or subsonic, nearly loss-free ballistic-like transport of electrons bound to lattice solitons (a form of electron surfing on acoustic waves) along crystallographic axes in two-dimensional anharmonic crystal lattices. First we study the structural changes a soliton creates in the lattice and the time lapse of recovery of the lattice. Then we study the behavior of one electron in the polarization field of one and two solitons with crossing pathways with suitably monitored delay. We show how an electron surfing on a lattice soliton may switch to surf on the second soliton and hence changing accordingly the direction of its path. Finally we discuss the possibility to control the way an excess electron proceeds from a source at a border of the lattice to a selected drain at another border by following appropriate straight pathways on crystallographic axes.

## 1 Formulation of the problem

In the present work we discuss the problem of control of electrons by acoustic lattice soliton excitations [1], a form of electron *surfing*, which may have different origins such as e.g. mechanical or electrical shocks generated by contacts of the tip of an electron field microscope with a suitable anharmonic crystal lattice layer. We consider systems of a few hundred atoms on a plane interacting with one or a few added, excess electrons. Earlier we have discussed the interaction between electrons and strongly localized lattice excitations of soliton-type in one- (1d) and two-dimensional (2d) lattices [1–4]. For the electron dynamics we used the tight-binding approximation (TBA) and for the lattice particles a classical Hamiltonian albeit with the quantum Morse interactions. As a result of this mixed anharmonic classical-quantum TBA dynamics we could show that the electrons “like” to follow the trajectories of soliton-like excitations. In the 1d case we have predicted several interesting phenomena, in particular the “vacuum-cleaner” effect, i.e., the electron probability density is gathered by solitons which along their trajectory act as long range correlators [5]. Noteworthy is that these excitations move in general with *supersonic* velocity or velocities a bit below the sound velocity depending on the parameter values, on the initial conditions and on the electron-lattice interaction. This means that electrons

bound to lattice solitons (in short called *solelectrons*) can move ballistic-like with high velocities of more than 1 km/s in a crystalline medium hence velocities orders of magnitude higher than in standard conductors [6]. In the present work we propose some new features of such soliton-assisted transport and illustrate it by dynamic computer simulations on a triangular lattice. Around a passing soliton or solelectron the lattice experiences some reversible local disturbance creating a transient loss of crystallinity. After a finite time which is 5–10 time units in our examples the lattice returns to its ordered crystalline state. In this transitory time solitons which try to go through cannot survive due to the leaking of too much (linear) phonon radiation. This time delay could be used to advantage for a form of control of electron transport that mimics the channeled transport in a field effect transistor with, however, no need of an additional voltage. This is the novelty of our approach which brings a form of transport with a drastic reduction of losses and heat.

In order to explain in a qualitative way what is our problem let us first discuss without technical details the changes generated by a soliton in a lattice as illustrated in Figures 1 and 2. The technical details and the parameters will be discussed later. In Figure 1 we show the track of a running soliton excitation (in “bubble chamber representation”,  $\rho_{ex}$ ) which was created by pushing just one atom in the direction of the crystallographic axis  $x$ , each atom is assumed to be a ball-like Gaussian core electron density,  $\rho$ , centered at each corresponding site. We show the space

<sup>a</sup> e-mail: mgvelarde@pluri.ucm.es

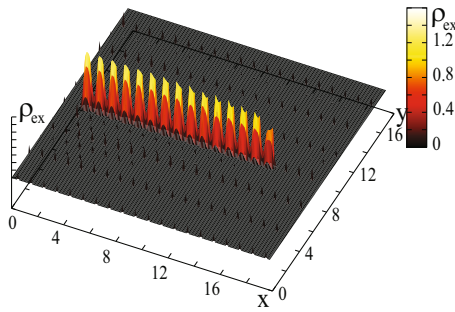


**Fig. 1.** Triangular Morse lattice. The soliton is excited by a strong kick (velocity  $v_0 = 2$  in units  $\sigma\omega_0$ ) imposed to one lattice particle. A track of the excitation (in “bubble chamber representation”,  $\rho_{ex}$ ) of the running soliton density is represented in a cumulative sequence of snapshots as time proceeds during the time interval  $\Delta t = 5$ . Parameter values:  $N = 400$ ,  $b\sigma = 4$ ,  $\lambda = 0.3\sigma$ .

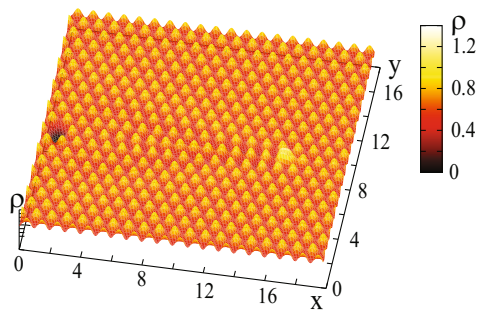


**Fig. 2.** Triangular Morse lattice with a soliton generated at  $t = 0$  by a strong kick at the left border. The kick corresponds to a pulse velocity  $v_0$  (and a rather high energy  $(b\sigma)^2 v_0^2 / 2$  measured in units  $2D$ ) imposed to one lattice particle located not far from the left border here the 2nd atom in the row. The density of the atomic core electrons is presented as a snapshot at time  $t = 5$  after launching the soliton. Further details are provided in the main text. Parameter values:  $N = 200$ ,  $b\sigma = 4$ ,  $v_0 = 2$ .

and time evolution of the initial soliton density peak for the time interval  $\Delta t = 5$  (measured in units of  $1/\omega_0$ , where  $\omega_0$  is the linear frequency of lattice oscillations around the rest point). The soliton which is moving along a crystallographic axis was excited by a strong pulse of velocity  $v_0$  imposed at  $t = 0$  to the 2nd atom in the 10th row with rather high energy  $mv_0^2/2$ . The high-energetic soliton excited this way is quite long lasting in its motion along the chosen crystallographic axis. Transverse excitations and scattering do not play a significant role in the interval of observation (5 time units). In Figure 2 we show a snapshot of the lattice state at the time  $t = 5$  after the kick. The snapshot of the lattice state shows that the head of the soliton (recall core electron density,  $\rho$ ) is already at position 15-16 but the changes in the lattice are still seen along the path. The very left dark points remember the initial kick. What follows is the dynamic tail of the moving soliton which excites linear oscillations, i.e. phenomena belonging to the phonon band [7]. The soliton as it travels disturbs the lattice. Only after a finite time which is about

5 time units in our example the lattice returns to the originally ordered crystalline state. In the transitory time we can say that locally the lattice is in a non-crystalline state and unable to allow solitons to maintain their path or survive. Any second soliton which would try to cross the trace of a soliton in the delay time will get stuck. Let us show how this effect makes possible to control the path of an electron from a given source to a given drain like in a transistor structure, as earlier indicated. Nowadays the world of atomically thin 2D (layered) materials is becoming of extraordinary interest (adequately coated GaAs layers,  $\text{LiNbO}_3/\text{SiO}$  structures, graphene/strained and otherwise, graphane or hydrogenated graphene, silicene or the silicon analogue of graphene, hexagonal boron nitride, tungsten diselenite, molybdenum disulfide, stanene, and other Van der Waals heterostructures) [8–12].

## 2 The dynamical model for lattice and electrons

The Hamiltonian of our 2d lattice consists of a classical lattice component  $H_a$ , and the contribution of the electrons  $H_e$ , which includes the interactions with the lattice deformations. For the lattice part, the Hamiltonian is

$$H_a = \frac{m}{2} \sum_n v_n^2 + \frac{1}{2} \sum_{n,j} V(r_n, r_j). \quad (1)$$

The subscripts locate the atoms all with equal mass,  $m$ , at lattice sites and the summations run from 1 to  $N$ . We assume that effects connected with polarization and polaron effects are small. The atoms repel each other exponentially and attract each other with weak dispersion forces [1,13,14]. The characteristic length determining equilibrium distance between the particles in the lattice is  $\sigma$  which is used as the length unit. Using the relative distance  $r = |r_n - r_j|$  we introduce the Morse potential [1,13,14]:

$$V(r) = D \{ \exp[-2b(r - \sigma)] - 2 \exp[-b(r - \sigma)] \}. \quad (2)$$

By imposing the cutoff of the potential at  $1.5\sigma$ , we exclude unphysical cumulative interaction effects arising from the influence of lattice units outside the first neighborhood of each atom [3,4]. To study the nonlinear excitations of the lattice and the possible electron transport in a lattice in the simplest approximation it is sufficient to know the coordinates of the lattice (point) particles at each time and the interaction of lattice deformations with electrons. Coordinates of particles are obtained by solving the equations of motion of each particle under the influence of all possible forces. The latter may also include very weak friction and random forces that can be accounted by a Langevin model. For convenience in the 2d lattice dynamics rather than using  $x, y$ , we use complex coordinates  $Z = x + iy$ , where  $x$  and  $y$  are Cartesian coordinates. Then the initial classical Newton deterministic equations corresponding to the lattice Hamiltonian (1) yield to a Langevin dynamics

for the lattice units

$$\frac{d^2 Z_n}{dt^2} = \sum_k F_{nk}(|Z_{ik}|)z_{nk} + \left[ -\gamma \frac{dZ_n}{dt} + \sqrt{2D_v} (\xi_{nx} + i\xi_{ny}) \right], \quad (3)$$

where index  $n$  identifies a particle among all  $N$  particles of the ensemble,  $\gamma$  is a friction coefficient,  $D_v$  defines the intensity of stochastic forces,  $\xi_{n,x,y}$  denotes statistically independent generators of the Gaussian noise. Further  $Z_{nk} = Z_n - Z_k$  and  $z_{nk} = (Z_n - Z_k)/|Z_n - Z_k|$  is the unit vector defining the direction of the interaction force  $F_{nk}$ , corresponding to the Morse potential, between the  $n$ th and the  $k$ th atoms in the lattice. To have dimensionless variables we consider the spatial coordinates rescaled with  $\sigma$ . Time is normalized to the inverse frequency of linear oscillations near the minimum of the Morse potential well,  $\omega_0^{-1}$ , whereas energy is scaled with  $2D$ . In view of the above only those lattice units with coordinates  $Z_k$ , satisfying the condition  $|Z_n - Z_k| < 1.5$ , are taken into account in the sum in equation (3). In computer simulations the interaction of lattice units is considered to take place inside a rectangular cell  $L_x L_y$  with periodic boundary conditions and depending on the symmetry of an initial distribution of units and their number  $N$ . The initial condition is defined by the distribution corresponding to the minimum of potential energy for an equilibrium state of a *triangular* lattice  $20 \times 20$ . For visualization and tracking the atomic electron densities we model the atoms as little spheres with “core” electrons represented by a Gaussian distribution centered at each lattice site:

$$\rho(Z, t) = \sum_{|Z - Z_n(t)| < 1.5} \exp \left[ -\frac{|Z - Z_n(t)|^2}{2\lambda^2} \right]. \quad (4)$$

Using data about trajectories of particles  $Z_n(t)$  and their velocities we can calculate the lattice atom distribution  $\rho(Z, t)$ .

From the length of the cumulative path and the time interval we may estimate the velocity. It appears that this strong local compression moves with velocity exceeding the sound velocity with a lifetime of at least several time units. In the 2d triangular Morse lattice  $v_{sound}$  is slightly above 1 in our units. These features point to soliton-like behavior. Indeed, they move a few picoseconds with nearly unaltered profile and just this robustness is the reason that we can identify them with the proposed visualization method. Losses due to scattering and radiation of linear waves are quite low, due to the nearly integrable character of the problem. Note that the 2d solitons observed here, are similar to the so-called lump solutions of the Kadomtsev-Petviashvili equation [15,16].

In the following section we will show that the nanosize of our 2d-structure makes possible the existence of electric structures due to the interactions of the electrons with the nonlinear lattice deformations, similar to those seen in the 1d-case. Let us now focus on the role played by one or several non-interacting electrons embedded into the atomic

lattice, maybe as a result of doping or injection. As long ago noted by Davydov [17] a soliton is connected with a deformation density of the lattice along its path. In order to study the evolution of the quantum states of the additional electrons interacting with the atoms in the 2d-lattice, we use the tight-binding approximation (TBA) [18,19]

$$H_{el} = \sum_n E_n c_n^\dagger c_n + \sum_{n,n'} t_{n,n'}(\mathbf{r}_{n'} - \mathbf{r}_n) c_{n'}^\dagger c_n, \quad (5)$$

where  $t_{n,n'}$  is the transition matrix. Here we assume only one quantum state of electrons per site and transitions between  $\mathbf{r}_n$  and  $\mathbf{r}_{n'}$ . The transition matrix elements  $t_{n,n'}$  depend on the atomic distances,  $t_{n,n'} = t(\mathbf{r}_{n'} - \mathbf{r}_n)$ . Following Launay and Verdaguer [18] and Slater [20] we take an exponential expression for the transition probabilities

$$t_{n,n'} = V_0 \exp[-\alpha_h |\mathbf{r}_n - \mathbf{r}_{n'}|]. \quad (6)$$

The range parameter  $\alpha_h$  can be related to the tunneling probability that decreases exponentially with distance. A full quantum mechanical description of the electrons in the field of the fast changing lattice is rather difficult. To simplify this situation we may assume that the electrons allow a Markov description, modeled as a Monte Carlo dynamics [3,4]. This is in particular useful for high enough temperatures. Here however we work in the region of low temperatures, where the temperature influence is negligible, and use as model for the electron dynamics  $N$  Schrödinger equations in TBA for the complex amplitudes  $c_n$  given in dimensionless units by:

$$i \frac{dc_n}{dt} = \epsilon_0 c_n - \tau \exp[\alpha b \sigma] \sum_{|Z_n - Z_m| < 1.5} c_m \exp(-\alpha |Z_n - Z_m|), \quad (7)$$

where the amplitude belongs to the quantum state of atom  $n$  ( $n = 1, \dots, N$ ) located at  $Z_n = x_n + iy_n$ , further we use  $\tau = V_0/\hbar\omega_0$ ,  $\alpha = \alpha_h \sigma$ . We do not assume any regular order of the atoms, except at  $t = 0$ , where a triangular lattice configuration is assumed. The electrons may hop between the lattice sites, the constant energy  $\epsilon_0$  of electrons at lattice site  $n$  is irrelevant for the dynamics. As earlier noted the sum  $n \neq m$  in the transition term is restricted over pairs with distance smaller than  $1.5\sigma$ . Quantum transitions occur preferentially between nearby lattice sites. Then the set of evolution equations equations (1)–(7) reduce to equation (7) and the complex Newtonian (or Langevin) equations:

$$\begin{aligned} \frac{d^2 Z_n}{dt^2} = & \sum_{|Z_n - Z_m| < 1.5} \left[ \exp(b\sigma - |Z_n - Z_m|) \right. \\ & \times (1 - \exp(b\sigma - |Z_n - Z_m|) \\ & + 2\alpha V \exp[\alpha(b\sigma - |Z_n - Z_m|)]) \\ & \left. \times \text{Re}(c_n c_m^*) \right] \frac{Z_n - Z_m}{|Z_n - Z_m|} \end{aligned} \quad (8)$$

( $V = V_0/(2D)$ ). We assume that in our case the mechanical excitations are strong enough to dominate the evolution of the system and hence the feedback from the electron dynamics to the lattice dynamics, i.e. the polaron effects, are small [21].

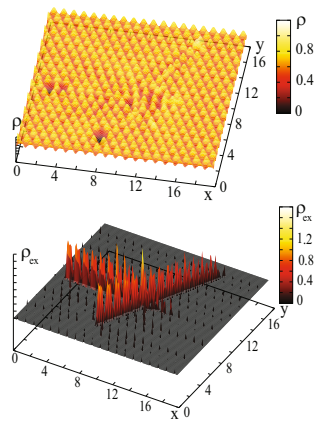


**Fig. 3.** Crossing soliton excitations in a 2d Morse lattice. Soliton and electron initially placed at the left border travel together as a solectron bound state along the given axis. The two panels correspond to crossing with a second soliton arriving from the lower border at an angle of  $60^\circ$ . Above is a snapshot of the lattice deformation state at  $t = 6$  and below, in cumulative sequence of snapshots, the extra compression density (in “bubble chamber representation”,  $\rho_{ex}$ ) for the time interval  $t = 0-6$ . The difference in paths, a way of monitoring delay, is about two  $\sigma$  units shorter for the second (“controller soliton”). Parameter values:  $N = 400$ ,  $b\sigma = 4$ ,  $v_0 = 1.5$ ,  $\tau = 10$ ,  $\alpha = 1$ ,  $V = 0.2$ .

### 3 Changing the path of a solectron by delayed interaction with a second soliton

Our idea of controlling the path of electrons is based on the properties of the deformations explained in the first section. One possibility is that just before launching (hence delayed in controllable way) a soliton/solectron along a crystallographic axis (which is here parallel to the lower  $x$ -axis border) we let another soliton (with same characteristics) start from the lower border at an angle with the trajectory of the former. The first soliton will stop for a while since it should arrive at a messy (non-crystalline) lattice region left by the other soliton. As the electron sitting on the first soliton starts being delocalized then the second crossing soliton gathers its electron probability density around its soliton polarization potential well thus recreating a new solectron which now travels at an angle relative to the trajectory of the former solectron. Another possibility is to simultaneously launch the second soliton from a point such that it is expected to travel a shorter path than the former. This is also a form of controllable delay. This is illustrated in Figures 3–5.

### 4 Controlling electron transport from source to drain

In the electron trapping process, the local lattice compressions significantly deform the potential landscape acting on added, excess electrons and create a moving *guiding* well or trap. In a piezoelectric crystal this would correspond to a traveling piezopotential like phenomena exhibited with surface acoustic waves [22–28]. There is also a

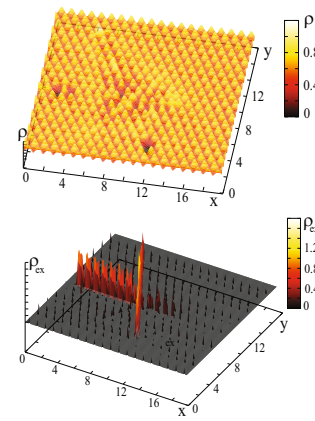


**Fig. 4.** The same dynamic computer simulation experiment as shown in Figure 3 is carried out with a crossing angle of  $120^\circ$ .

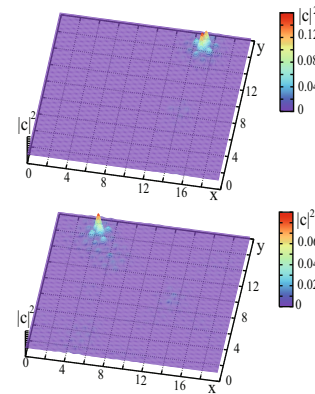


**Fig. 5.** Triangular Morse lattice. Snapshot of the final states of electron probability density,  $\sum |c_n|^2$ , after performing the experiment with crossing soliton excitations as seen in Figures 3 and 4. Note that soliton and electron were initially placed at the left border. Subsequently they travel together as a solectron bound state along the axis parallel to lower border ( $x$ -axis). After crossing the path of the soliton initiated from lower border the electron density moves to definite places (the drains) at the upper border. Which drain is targeted by the electron, depends on the direction ( $60^\circ$  – upper panel or  $120^\circ$  – lower panel) of the crossing (second) “controller soliton”.

feedback of the concentration of electron probability density on the lattice deformation which is small in our case. Indeed, in the supersonic case, for the given parameter values, this feedback is rather small, changing the results by less than a few percent [21] (see also [29–31]). Generally, the electrons tend to be trapped in the regions of maximal density of lattice points created by the local compressions and then forced to move dynamically bound to the soliton-like compressions which in 2d is favored along the crystallographic axes.

Figure 3 (respectively Fig. 4) shows a soliton moving left to right (bearing an electron). Without meeting an obstacle the electron will be carried along the crystallographic axis to the right border. However if the soliton encounters on its path as shown in Figure 3 (respectively Fig. 4) another (bare) soliton at an angle  $60^\circ$  (respectively

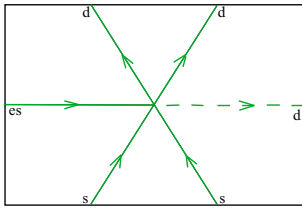


**Fig. 6.** Sketch of the proposed mechanism of electron control and transport from source to drain like in a field effect transistor. An electron and a soliton bound at the source (es) at the left border and two soliton emitters (s) at the lower border are displayed. Depending on which soliton dominates, the electron may be directed to any of the drains (d) at the right border or at the upper. Note that all crystallographic axes can be used to have a source (and soliton emitter) or a drain.

120°) a reorientation starts. As the former soliton cannot proceed forward due to the locally messy non-crystalline state in the lattice after having passed the second soliton crossing from below (which is similar to a local “melting”) then the latter dominates the dynamics. When the former soliton carries an added electron hence forming a solectron, then, as early noted, the electron tends to loose the bound state with it (its first partner) and is prone to be bound to the second, now dominant soliton, hence forming a new solectron. Consequently the suitably delayed or even simultaneous crossing of two solitons permits to bring an electron from a given source to a given drain either on its unperturbed first path or to another site like one near to the right upper corner (Fig. 3) or to the left upper corner (Fig. 4). The source-drain channel for the electron is naturally one of three crystallographic axes. The processes discussed here offer a novel way of controlling and transporting electrons from a given source to a given drain like in a field effect transistor. Figure 6 offers a sketch of the various possibilities for controlling the way of an electron from a source at the left border (es) to any of three possible drains (d) on the upper or on the right border.

The present computer experiments belong to a nanoscale concerning a few hundred atoms on a plane (with periodic boundary conditions) but they can be related to experiments on a larger scale with surface acoustic waves (SAW). Linear and nonlinear SAW propagating in a homogeneous elastic medium, piezoelectric, or otherwise, exhibit no dispersion. If the medium is nonlinear, as e.g. in *anharmonic* crystal lattices, an initial sinusoidal SAW can create higher harmonics which may grow without being inhibited by dispersion. Dispersion can be introduced by coating the medium with a thin film of another material with elastic and structural/mechanical properties different from those of the substrate. Then by an appropriate choice of the film thickness, the effects of *nonlinearity* and *dispersion* can balance each other thus sustaining solitons as long ago Nayanov and others observed [22–28]. Experiments have demonstrated the possibility of acoustic charge transport in semiconductor heterostructures by SAW [25,32,33]. As high amplitude SAW tend to deform to sawtooth shape and eventually break, the suggestion com-

ing from our theory is that for electron surfing, no matter the scale involved, solitons should be better carriers than linear waves, even if the latter are highly monochromatic. Finally, let us recall the mentioned recent extraordinary interest offered by the huge diversity of 2D layered materials.

The authors acknowledge fruitful discussions and correspondence with L. Cruzeiro, D. Hennig, A. Knorr and G. Röpke. They also wish to thank R.P.G. McNeil, C. Ford, T. Meunier and A. Wixforth for sharing with us their electron surfing experiments in piezoelectric GaAs layers and V.I. Nayanov for his enlightening description of SAW in nonlinearly elastic, piezoelectric LiNbO<sub>3</sub> layers where wave dispersion able to balance nonlinearity of the substrate is monitored by depositing, via evaporation, SiO films of suitable thickness. E.G. Wilson is also gratefully acknowledged for detailed information on his experiments on soliton-mediated charge motion in PDA crystals. This work was completed during a research stay of the authors at the Collaborative Research Center 910 of the Technical University in Berlin. The authors gratefully acknowledge Prof. Eckehard Schöll for hospitality and financial support.

## References

1. M. Toda, *Theory of Nonlinear Lattices*, 2nd edn. (Springer-Verlag, New York, 1989)
2. A.P. Chetverikov, W. Ebeling, G. Röpke, M.G. Velarde, *Eur. Phys. J. B* **87**, 153 (2014)
3. A.P. Chetverikov, W. Ebeling, M.G. Velarde, *Eur. Phys. J. B* **70**, 217 (2009)
4. A.P. Chetverikov, W. Ebeling, M.G. Velarde, *Eur. Phys. J. B* **80**, 137 (2011)
5. D. Hennig, A.P. Chetverikov, M.G. Velarde, W. Ebeling, *Phys. Rev. E* **76**, 046602 (2007)
6. M.P. Shaw, V.N. Mitin, E. Schöll, H.L. Grubin, *The Physics of Instabilities in Solid State Electron Devices* (Springer, Berlin, 1992)
7. M.G. Velarde, A.P. Chetverikov, W. Ebeling, S.V. Dmitriev, V.D. Lakhno, *Proc. Estonian Acad. Sci.* **64**, 396 (2015)
8. B. Radisavljevic, A. Radenovic, J. Brivio, V. Giacometti, A. Kis, *Nat. Nanotechnol.* **6**, 147 (2011)
9. A.C. Ferrari et al., *Nanoscale* **7**, 4598 (2015)
10. R. Hoffmann, *Angew. Chem. Int. Ed.* **52**, 93 (2013)
11. L. Tao, E. Cinquanta, D. Chiappe, C. Grazianetti, M. Fanciulli, M. Dubey, A. Molle, D. Akinwande, *Nat. Nanotechnol.* **10**, 227 (2015)
12. F.-F. Zhu, W.-J. Chen, Y. Xu, C.-I. Gao, D.-D. Guan, C.-H. Liu, D. Qian, S.-C. Zhang, J.-F. Jia, *Nat. Mater.* **14**, 1020 (2015)
13. J. Dancz, S.A. Rice, *J. Chem. Phys.* **67**, 1418 (1977)
14. T.J. Rolfe, S.A. Rice, J. Dancz, *J. Chem. Phys.* **70**, 26 (1979)
15. A.P. Chetverikov, W. Ebeling, M.G. Velarde, *Physica D* **240**, 1954 (2011)
16. A.A. Minzoni, N.F. Smyth, *Wave Motion* **24**, 291 (1996)
17. A.S. Davydov, *Solitons in Molecular Systems*, 2nd edn. (Reidel, Dordrecht, 1991)

18. J.-P. Launay, M. Verdaguer, *Electrons in Molecules. From Basic Principles to Molecular Electronics* (Oxford University Press, Oxford, 2013)
19. M.G. Velarde, J. Comp. Appl. Math. **233**, 1432 (2010)
20. J.C. Slater, in *Quantum Theory of Molecular and Solids. The Self-Consistent Field for Molecules and Solids* (McGraw-Hill, New York, 1974), Vol. 4
21. O.G. Cantu Ros, L. Cruzeiro, M.G. Velarde, W. Ebeling, Eur. Phys. J. B **80**, 545 (2011)
22. V.I. Nayanov, I.A. Vasilev, Sov. Phys. Solid State **25**, 1430 (1983)
23. V.I. Nayanov, J. Exp. Theor. Phys. Lett. **44**, 314 (1986)
24. A.P. Mayer, Phys. Rep. **256**, 237 (1995)
25. M. Streibl, A. Wixforth, J.P. Kotthaus, A.O. Govorov, C. Kadow, A.C. Gossard, Appl. Phys. Lett **75**, 4139 (1999)
26. A.P. Mayer, Ultrasonics **48**, 478 (2008)
27. Z. Insepov, E. Emelin, O. Kononenko, D.V. Roshchupkin, K.B. Tnyshtykbayev, K.A. Baigarin, Appl. Phys. Lett. **106**, 023505 (2015)
28. A. Vikström, Low Temp. Phys. **41**, 293 (2015)
29. J.S. Zmuidzinas, Phys. Rev. B **17**, 3919 (1978)
30. A. Ranciaro Neto, M.O. Sales, F.A.B.F. de Moura, Solid State Commun. **229**, 22 (2016)
31. A. Ranciaro Neto, F.A.B.F. de Moura, Commun. Nonlinear Sci. Numer. Simulat. **40**, 6 (2016)
32. S. Hermelin, S. Takada, M. Yamamoto, S. Tarucha, A.D. Wieck, L. Saminadayar, C. Bäuerle, T. Meunier, Nature **477**, 435 (2011)
33. R.P.G. McNeil, M. Kataoka, C.J.B. Ford, C.H.W. Barnes, D. Anderson, G.A.C. Jones, I. Farrer, D.A. Ritchie, Nature **477**, 439 (2011)